Available online at www.sciencedirect.com

ScienceDirect

Applied Mathematical Modelling 31 (2007) 2286–2298

APPLIED MATHEMATICAL MODELLING

www.elsevier.com/locate/apm

Modelling wax diffusion in crude oils: The cold finger device

S. Correra [a], A. Fasano [b], L. Fusi [b,*], M. Primicerio [b]

[a] *EniTecnologie, Via F.Maritano, 20097, San Donato Milanese, Milano, Italy*

[b] *I2T3 – c/o: Dipartimento di Matematica "U.Dini", Universitá di Firenze, Viale Morgagni 67/A, 50134 Firenze, Italy*

Received 1 December 2005; received in revised form 1 June 2006; accepted 4 September 2006
Available online 27 October 2006

Abstract

In this paper we show how to obtain wax diffusivity and solubility values in crude oils from deposition measurements in the cold finger device with stirring. Providing a rather accurate knowledge of such quantities is of great importance in predicting the wax deposition rate in pipelines. We present a mathematical model in which the physical quantities are assumed to be space-independent in the bulk region of the device, because of agitation, so that mass transport occur in relatively thin boundary layers. As a consequence the deposition phenomenon is accelerated with respect to the static device (see [S. Correra, A. Fasano, L. Fusi, M. Primicerio, F. Rosso. Wax diffusivity under given thermal gradient: a mathematical model, to appear on ZAMM]), shortening the duration of experiments. Comparison with some available laboratory measurements shows a satisfactory agreement and the values obtained are in the range of those usually adopted by practitioners.

1. Introduction

Waxy crude oils (WCOs) are mineral oils with high molecular weight paraffinic components (from C17 on) which below the so-called *Cloud Point* temperature (denoted by T_{cloud}) may separate as a wax phase, causing a series of severe problems during transportation along pipelines. One of the most important is certainly the formation of a solid deposit on pipeline walls, (*wax deposition*). This phenomenon is of crucial importance in the oil industry because it can cause the partial or total blockage of a line, causing production to decrease or halt.

Since pipeline blockage removal can be very expensive (for instance in submarine ducts) many industries are interested in having a good understanding of wax precipitation and deposition processes.

Laboratory devices like test loops or the cold finger (a thermally controllable device used to simulate deposition in static and dynamic conditions, see [1–4] are set up in order to simulate wax deposition in pipelines. They can be used both for predicting the amount of deposit under specific physical conditions and for determining the main physical parameters like wax solubility and diffusivity.

* Corresponding author.
E-mail address: fusi@math.unifi.it (L. Fusi).

0307-904X/$ - see front matter
doi:10.1016/j.apm.2006.09.007

Wax deposition is the result of different mechanical and thermal processes that occur under specific physical conditions (for a general overview we refer the reader to [5,6]). Here we will investigate deposition in the cold finger device (with stirring) when deposition is due only to molecular diffusion, a deposition mechanism induced by the presence of a thermal gradient in the oil (see [5]).

Of course, the phenomenon differs from the one observed in the static case (see [1,2]). This is basically due to the fact that agitation homogenizes all the relevant physical quantities, so that temperature and concentrations can be considered uniform except for some boundary layers near the walls.

The experimental apparatus consists of a cylindrical thermostatic bath in which the oil is kept at a desired fixed temperature until a metallic probe (maintained below the cloud point) is introduced and placed at the axis of the cylinder. More precisely, the oil is initially charged in the bath and warmed over the cloud point. Then its temperature is gradually lowered to a temperature T_e which will be kept fixed throughout the experiment. At this point the cold probe (which is at temperature $T_i < T_e$ with $T_i < T_{cloud}$) is co-axially inserted in the bath. Simultaneously a mixer placed at the bottom begins to stir the oil. When the vicinity of the cold finger is saturated by wax the presence of a thermal gradient near the cold wall (in the bulk, temperature is homogeneized because of the stirring) induces a concentration gradient. The latter, by Fick's law, produces mass transfer of dissolved wax towards the cold finger, and thus deposition.

In [2] we have studied the case when the oil is static (no stirring). In that case we have observed that, in case of initial complete saturation, the system evolves through three stages: (i) complete saturation, (ii) partial desaturation, (iii) complete desaturation, the second stage being characterized by the presence of a desaturation front moving from the warm wall towards the cold finger.

In the stirred case, because of homogenization, stage two does not exist and the system evolves from complete saturation to complete desaturation. This is because in the bulk the parameters describing the wax content are independent of the radial coordinate.

In this paper we will present and analyze a mathematical model that allows the prediction of wax diffusivity and solubility starting from deposition measurements. Conversely, the model allows us to predict the amount of deposit once such parameters are known.

On the basis of available experimental data we will see that the wax diffusivity values that will be obtained are in the range of the ones usually found in the literature (derived from classical correlations).

In this conceptual model we will suppose that the following simplifying assumptions are satisfied:

(i) deposition is due only to molecular diffusion,
(ii) the saturation concentration C_s (solubility) is a linear function of temperature T,
(iii) oil and wax have the same constant density ρ (typically 800 kg/m^3, see [6]).

We denote by c_{tot}, c^*_{tot}, c, G, T_{cloud} total wax concentration, initial total wax concentration, dissolved wax concentration, segregated wax concentration and cloud point respectively. Under the assumption that thermodynamical equilibrium between dissolved and segregated phase is instantaneously reached we write

$$c_{tot} = c + G, \tag{1.1}$$

$$G = [c - C_s(T)]_+. \tag{1.2}$$

Moreover, since $C_s(T)$ represents the amount of wax that can be dissolved at temperature T, we have

$$c^*_{tot} = C_s(T_{cloud}). \tag{1.3}$$

2. The mathematical model

We present here the mathematical model for wax deposition for the cold finger with stirring. Due to the large thermal diffusivity, we assume that an equilibrium temperature profile is reached instantaneously. The latter is characterized by a bulk zone at constant temperature T_b and two boundary layers near the walls.

The system evolves through two stages. In the first stage the deposition rate is constant and mass grows linearly with time, while in the second stage the deposition rate tends asymptotically to zero (exponential decay).

Mass diffusion takes place in the boundary layer near the cold wall, where a thermal gradient is present. As long as the bulk remains saturated the loss of wax due to deposition is balanced by dissolution of segregated wax. When desaturation is achieved the deposition rate starts to decrease and the wax concentration in the bulk tends to the saturation concentration corresponding to the cold finger temperature.

The deposit is formed by oil and wax and the wax fraction ϕ is assumed to be independent of time. The value of ϕ is expected to be larger than in the static device and closer to the ones found in pipeline deposits [7]. It will be shown that ϕ has no influence on the final determination of wax diffusivity.

2.1. Thermal profile

Let us denote by $r = R_i$ and $r = R_e$ the cold and warm wall radii. As stated above temperature is constant except in two boundary layers near the walls. The thickness of the boundary layers is constant and denoted by $r_i - R_i$ (cold wall) and $R_e - r_e$ (warm wall). The bulk temperature T_b is uniform, while in the boundary layers T has a steady profile

$$T(r) = T_i + \frac{T_b - T_i}{\ln\left(\frac{r_i}{R_i}\right)} \ln\left(\frac{r}{R_i}\right), \quad R_i \leqslant r \leqslant r_i, \tag{2.1}$$

$$T(r) = T_e + \frac{T_b - T_e}{\ln\left(\frac{r_e}{R_e}\right)} \ln\left(\frac{r}{R_e}\right), \quad r_e \leqslant r \leqslant R_e, \tag{2.2}$$

where $T_i < T_e$ are the temperatures at the inner and outer wall respectively (see Fig. 1).

To evaluate the thickness of the boundary layers we consider the heat flux per unit height through the boundary layer $R_i \leqslant r \leqslant r_i$

$$q_i = 2\pi R_i h_i (T_b - T_i), \tag{2.3}$$

where h_i is the heat transfer coefficient at the cold wall. The flux q_i has to be equal to

$$2k\pi R_i \frac{dT}{dr}(R_i), \tag{2.4}$$

where k is the thermal conductivity and

$$\frac{dT}{dr}(R_i) = \frac{T_b - T_i}{\ln\left(\frac{r_i}{R_i}\right)} \frac{1}{R_i} \tag{2.5}$$

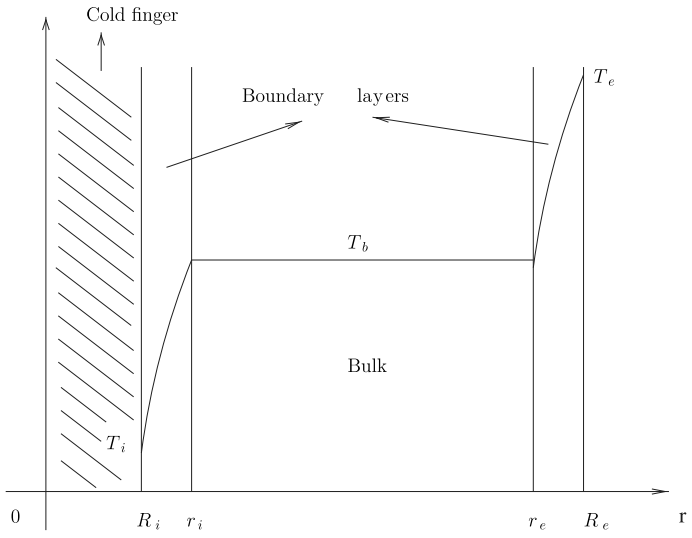

Fig. 1. Geometry of the system and thermal profile.

is the thermal gradient at $r = R_i$. Imposing equality of (2.3) and (2.4) we get

$$r_i = R_i \exp\left\{\frac{k}{h_i R_i}\right\}, \tag{2.6}$$

which relates the boundary layer thickness to the heat transfer coefficient h_i. In an analogous way we can show that

$$r_e = R_e \exp\left\{-\frac{k}{h_e R_e}\right\}, \tag{2.7}$$

where h_e is the heat transfer coefficient at the warm wall. We may assume $h = h_i = h_e$ where h can be computed (see [3]) using

$$h = \frac{k}{R_i^{1-m}}\left(\frac{\rho\omega(R_e - R_i)}{2\mu}\right)^m, \tag{2.8}$$

ω being the rotational speed, μ the viscosity and $m = 0.628$. Assuming typical values (see [8])

$$\mu = 30 \text{ cP}, \quad \omega = 500 \text{ rpm}, \quad \rho = 800 \ \frac{\text{kg}}{\text{m}^3}, \tag{2.9}$$

$$k = 0.1 \ \frac{\text{W}}{\text{m K}}, \quad R_i = 0.017 \text{ m}, \quad R_e = 0.043 \text{ m}, \tag{2.10}$$

we get

$$h = 215.14 \ \frac{\text{W}}{\text{m}^2 \text{ K}}, \tag{2.11}$$

$$r_i - R_i = 4.7 \times 10^{-4} \text{ m}, \tag{2.12}$$

$$R_e - r_e = 4.6 \times 10^{-4} \text{ m}. \tag{2.13}$$

The bulk temperature T_b can be obtained by imposing that the incoming heat flux entering $r = R_e$ is equal to the outgoing heat flux in $r = R_i$, that is

$$R_i(T_b - T_i) = R_e(T_e - T_b).$$

We obtain

$$T_b = \frac{R_e T_e + R_i T_i}{R_e + R_i}. \tag{2.14}$$

In expressions (2.1) and (2.2) T_b has to be replaced by (2.14), and r_i, r_e by (2.6) and (2.7). The complete temperature profile becomes

$$T = T_i + \frac{hR_iR_e}{k}\frac{(T_e - T_i)}{(R_e + R_i)} \ln\left(\frac{r}{R_i}\right), \quad R_i \leqslant r \leqslant r_i, \tag{2.15}$$

$$T_b = \frac{R_e T_e + R_i T_i}{R_e + R_i}, \quad r_i \leqslant r \leqslant r_e, \tag{2.16}$$

$$T = T_e + \frac{hR_iR_e}{k}\frac{(T_e - T_i)}{(R_e + R_i)} \ln\left(\frac{r}{R_e}\right), \quad r_e \leqslant r \leqslant R_e. \tag{2.17}$$

2.2. Evolution of the segregated phase and estimate of the desaturation time

From the assumption that C_s depends linearly on T (see [2] for a justification), we write

$$C_s(T) = C_s(T_i) + b_w(T - T_i), \tag{2.18}$$

where the parameter b_w can be obtained using asymptotic mass measures. After a sufficiently long time (asymptotic stage) the dissolved wax concentration gradient becomes negligible and the dissolved wax concentration tends to $C_s(T_i)$. Thus we can write the following relation

$$m_{w\infty} = m_\infty \phi = (c^*_{tot} - C_s(T_i)) \frac{(R_e^2 - R_i^2)}{2R_i}, \tag{2.19}$$

where m_∞ is the asymptotic deposit (per unit surface) and $m_{w\infty}$ is the asymptotic mass of wax in the deposit. From the knowledge of ϕ and of the two measures m^1_∞, m^2_∞ (or alternatively from $m^1_{w\infty}$, $m^2_{w\infty}$) relative to two different cold finger temperatures T_1, T_2, from (2.18) and (2.19) we get

$$\frac{[m^1_{w\infty} - m^2_{w\infty}]2R_i}{(R_e^2 - R_i^2)(T_2 - T_1)} = \phi \underbrace{\frac{[m^1_\infty - m^2_\infty]2R_i}{(R_e^2 - R_i^2)(T_2 - T_1)}}_{=b} = \frac{C_s(T_2) - C_s(T_1)}{T_2 - T_1} = \phi b = b_w. \tag{2.20}$$

Notice that this formula does not contain the initial concentration c^*_{tot}.

Because of stirring, the segregated wax concentration G can be considered to be spatially uniform and we shall write $G = G(t)$. Let us suppose that the solution is initially saturated, that is $c^*_{tot} > C_s(T_e)$.

The thermal gradient in the region $R_i < r < r_i$ will induce the migration of dissolved wax towards the cold finger. When dissolved wax reaches the cold surface it segregates and adheres to the surface forming a solid deposit.[1] At the same time G is depleted because the segregated phase is dissolved to replace the wax that has been deposited.

Mass growth rate (per unit surface) at the cold wall is given by

$$\dot m_w = D_w b_w \left.\frac{dT}{dr}\right|_{r=R_i} = \phi \dot m = D_w \phi b \left.\frac{dT}{dr}\right|_{r=R_i}, \tag{2.21}$$

where D_w is the wax diffusivity[2] and

$$\left.\frac{dT}{dr}\right|_{R_i} = \frac{hR_e}{k} \frac{(T_e - T_i)}{(R_e + R_i)} \tag{2.22}$$

is obtained from (2.15). Mass balance is given by

$$\pi \dot G (R_e^2 - R_i^2) = -2\pi R_i D_w b_w \frac{hR_e}{k} \frac{(T_e - T_i)}{(R_e + R_i)}. \tag{2.23}$$

The left hand side of (2.23) represents the rate at which segregated phase is dissolved, while the right hand side describes the deposition rate (both per unit height of the cylinder). Integrating (2.23) with the initial datum $G(0) = G_0 = c^*_{tot} - C_s(T_b) < \rho$ we get

$$G(t) = G_0 - Bt,$$

where

$$B = \frac{2D_w b_w h R_i R_e}{k} \frac{(T_e - T_i)}{(R_e + R_i)(R_e^2 - R_i^2)}.$$

The desaturation time t_0 is obtained imposing $G(t_0) = 0$, that is

$$t_0 = \frac{G_0}{B}. \tag{2.24}$$

[1] From experimental measures (see [1,8]) we know that the thickness of the deposit does not appreciably modify the geometry of the system. When dealing with G we may reasonably identify r_i and r_e with R_i and R_e, since the thickness of the boundary layers are much smaller than the gap $R_e - R_i$.

[2] We remark that the ratio $\dot m_w / b_w$ (and hence D_w) is the same as the ratio $\dot m / b$ evaluated using the mass of the deposit with oil inclusion. Thus the coefficient ϕ has no influence in the computation of D_w.

2.3. Evolution of solute concentration c

Recall that $c_{tot} = G + c$. Due to agitation the solute will be uniformly distributed in the bulk and we write $c = c(t)$, in the global balance neglecting the slight (and opposite) corrections in boundary layers. During the "saturation" interval $[0, t_0]$ $c = C_s(T_b)$, with T_b given by (2.14). For $t > t_0$ the solution is unsaturated ($G = 0$, $c = c_{tot}$ in the bulk) and the mass transport law (2.21) has to be changed to account for the effects of depletion (see [7] p. 99). Depletion, i.e. wax transfer from the oil to the deposit, will be considered as the only mechanism driving to the asymptotic limit, neglecting the influence of the deposit on the geometry and on the the thermal field.

We denote the asymptotic value of the solute concentration by $c_\infty =: C_s(T_i)$. Mass growth rate (per unit surface) at the cold wall is

$$\dot{m}_w = \lambda(c - c_\infty), \tag{2.25}$$

where λ is a positive parameter (with the dimension of a velocity) to be determined. Mass balance is expressed by

$$\dot{c}\pi(R_e^2 - R_i^2) = -2\pi R_i \lambda(c - c_\infty). \tag{2.26}$$

Since at time $t = t_0$ we have $c(t_0) = C_s(T_b)$, integrating equation (2.26) we obtain

$$c(t) = c_\infty + (C_s(T_b) - c_\infty)\exp\left\{-\frac{2\lambda R_i}{(R_e^2 - R_i^2)}(t - t_0)\right\}, \tag{2.27}$$

that provides the solute concentration for $t \geqslant t_0$. Obviously (2.27) requires the knowledge of c_∞, $C_s(T_b)$ and λ. Total wax concentration can be written in the following way:

$$c_{tot}(t) = \begin{cases} G(t) + C_s(T_b), & 0 \leqslant t \leqslant t_0 \\ c(t), & t \geqslant t_0 \end{cases} \tag{2.28}$$

The function c_{tot} is continuous in $t = t_0$. In the next section we will see how to determine λ.

2.4. The parameter λ

Extending the validity of (2.25) to the saturation stage amounts to requiring that $c_{tot}(t)$, given by (2.28), is continuously differentiable in $t = t_0$. Accordingly, we impose

$$\dot{G}(t_0) = \dot{c}(t_0),$$

that is (see (2.23) and (2.26))

$$\frac{2D_w b_w h R_i R_e (T_e - T_i)}{k(R_e + R_i)(R_e^2 - R_i^2)} = \frac{2R_i\lambda(C_s(T_b) - c_\infty)}{(R_e^2 - R_i^2)}. \tag{2.29}$$

Recalling (2.14) and (2.18) we get

$$C_s(T_b) - c_\infty = \frac{b_w R_e (T_e - T_i)}{(R_e + R_i)}, \tag{2.30}$$

which substituted into (2.29) provides

$$\lambda = \frac{D_w h}{k}. \tag{2.31}$$

The plot of $c_{tot}(t)$ will be like the one shown in Fig. 2, with a linear behaviour up to the desaturation time t_0 and with an exponential decay for subsequent times.

Obviously the plot in Fig. 2 shows the evolution of the solute concentration as well. We notice that the latter is $C_s(T_b)$ up to time $t = t_0$ and then decreases exponentially to c_∞.

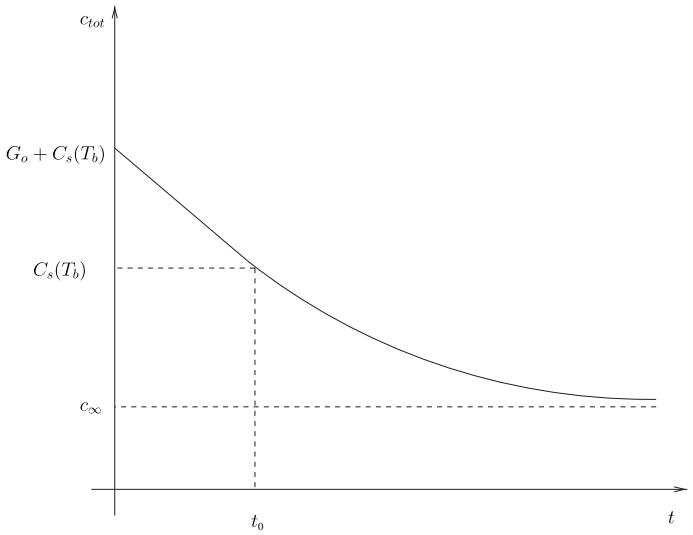

Fig. 2. Total wax concentration as a function of time.

2.5. The deposit and its evolution

Let us now consider the formation of the solid deposit layer on the cold wall. Denoting, as usual, by $m_w(t) = \phi m(t)$ the deposited wax mass per unit surface ($m(t)$ is the total deposited mass), we have

$$\dot{m}_w = D_w b_w \left.\frac{\partial T}{\partial r}\right|_{R_i} = \frac{D_w b_w h R_e}{k}\frac{(T_e - T_i)}{(R_e + R_i)} = \lambda(C_s(T_b) - c_\infty), \quad 0 \leqslant t \leqslant t_0, \tag{2.32}$$

$$\dot{m}_w = \lambda(C_s(T_b) - c_\infty)\exp\left\{-\frac{2\lambda R_i}{(R_e^2 - R_i^2)} \quad (t - t_0)\right\}, \quad t > t_0, \tag{2.33}$$

where the right hand sides of (2.32), (2.33) are the mass fluxes for the saturated and unsaturated stages respectively. Integrating (2.32) with the initial datum $m_w(0) = 0$ we find

$$m_w(t) = \lambda(C_s(T_b) - c_\infty)t, \quad 0 \leqslant t \leqslant t_0, \tag{2.34}$$

that indicates that the deposit grows linearly with time during the interval $[0, t_0]$. At the desaturation time t_0, we have (see (2.24) and (2.30))

$$m_w(t_0) = \frac{[c^*_{tot} - C_s(T_b)](R_e^2 - R_i^2)}{2R_i}. \tag{2.35}$$

Integrating (2.33) with the initial datum $m_w(t_0)$ we obtain

$$m_w(t) = m_w(t_0) + \frac{(R_e^2 - R_i^2)(C_s(T_b) - c_\infty)}{2R_i}\left[1 - \exp\left(-\frac{2\lambda R_i}{R_e^2 - R_i^2}(t - t_0)\right)\right]. \tag{2.36}$$

From (2.35) and from (2.36) we see that the asymptotic value $m_{w\infty}$ of deposited mass per unit surface is

$$m_{w\infty} = \frac{[c^*_{tot} - c_\infty](R_e^2 - R_i^2)}{2R_i} = \frac{[c^*_{tot} - C_s(T_i)](R_e^2 - R_i^2)}{2R_i} = \frac{b_w(T_{cloud} - T_i)(R_e^2 - R_i^2)}{2R_i}, \tag{2.37}$$

as stated in (2.19). The plot of deposited mass of wax as a function of time is sketched in Fig. 3. The curve shows a linear growth up to time t_0 and then it tends asymptotically to $m_{w\infty}$. The total mass of deposit m is obtained dividing m_w by ϕ.

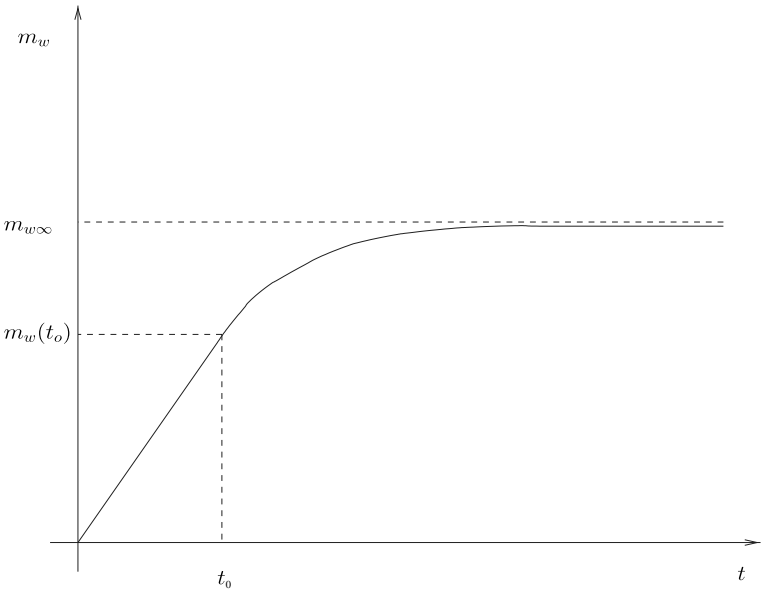

Fig. 3. Deposit as a function of time.

3. Comparison with experimental data

Here we determine b_w and D_w from some laboratory measurements and we compare our model with available data. In Fig. 4 some deposition measurements and wax fraction of the deposit obtained with a cold finger with stirring are reported. The experimental data are taken from [3] and represent the total deposited mass m and the wax fraction ϕ at 16 h, for some temperature difference $\Delta T = T_b - T_i$.

In all experiments bulk temperature is kept constant

$$T_b = 313.5 \text{ K},$$

varying the thermal gradient in the boundary layers. Fig. 4 refers to four different values of the difference $\Delta T = T_b - T_i$

$$\Delta T = 4.4 \text{ K}, \quad \Delta T = 8.3 \text{ K}, \quad \Delta T = 13.8 \text{ K}, \quad \Delta T = 25 \text{ K}. \tag{3.1}$$

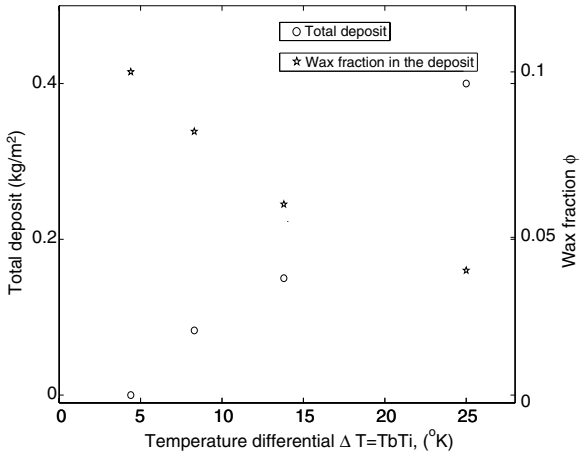

Fig. 4. Deposited mass m and wax fraction ϕ as a function of $\Delta T = T_b - T_i$. Measurements are taken after 16 h.

The cloud point is

$$T_{\text{cloud}} = 320.2 \text{ K},$$

the inner and outer radius of the cold finger are

$$R_{\text{i}} = 0.017 \text{ m}, \quad R_{\text{e}} = 0.043 \text{ m}.$$

3.1. Evaluation of b_w through asymptotic mass measures

In Fig. 4 the wax fraction in the deposit is also plotted, so that we know the actual mass of wax deposit m_{w}. The parameter b_{w} can be evaluated by means of (2.20) in the following way. We consider

$$\Delta T^0 = T_{\text{b}} - T_0,$$
$$\Delta T^1 = T_{\text{b}} - T_1,$$

where T_0 and T_1 are two different temperatures of the cold finger. We have

$$\Delta T^1 - \Delta T^0 = T_0 - T_1.$$

From (2.20)

$$b_{\text{w}} = \frac{[m^1_{\text{w}\infty} - m^0_{\text{w}\infty}]2R_{\text{i}}}{(R^2_{\text{e}} - R^2_{\text{i}})(\Delta T^1 - \Delta T^0)}. \tag{3.2}$$

The question of how to exploit the available experimental data of Fig. 4 in formula (3.2) is rather delicate, since it is never specified if the duration of the experiment is long enough to achieve the asymptotic values of the deposited mass or, on the contrary, is short enough to fall in the linear regime. We stress that from our arguments the correct experimental procedure, which should lead to an easy determination of both b_{w} and D_{w}, becomes clear: for each fixed ΔT various measures should be taken at different times in such a way that the duration of the linear deposition regime and the asymptotic value of the deposited mass can be deduced with sufficient accuracy.

The best we can do with the data at our disposal for deducing b_{w} is to select the data corresponding to $\Delta T^0 = 13.8$ K and $\Delta T^1 = 25$ K, for which the measured deposited mass m^0_{w}, m^1_{w} after 16 h are likely to be close to the asymptotic values $m^0_{\text{w}\infty}$, $m^1_{\text{w}\infty}$. Thus it is reasonable to expect that using in (3.2) the difference $m^1_{\text{w}} - m^0_{\text{w}}$ in place of $m^1_{\text{w}\infty} - m^0_{\text{w}\infty}$ does not produce a significant error. From the data of Fig. 4 relatively to $\Delta T^1 = 25$ K, $\Delta T^0 = 13.8$ K,

$$\Delta T^1 = 25 \text{ K} \quad \rightarrow \quad m^1_{\text{w}} = 0.016 \ \frac{\text{kg}}{\text{m}^2},$$
$$\Delta T^0 = 13.8 \text{ K} \quad \rightarrow \quad m^0_{\text{w}} = 0.0096 \ \frac{\text{kg}}{\text{m}^2}.$$

Thus, from (3.2)

$$b_{\text{w}} = 0.014 \ \frac{\text{kg}}{\text{m}^3 \text{ K}}. \tag{3.3}$$

Although the starting point of this procedure is affected by the possible error in the estimation of the difference $m^1_{\text{w}\infty} - m^0_{\text{w}\infty}$, we can eventually evaluate the correctness of the procedure by using formula (3.10) below with the estimated value of b_{w} to obtain the theoretical values of $m^0_{\text{w}\infty}$, $m^1_{\text{w}\infty}$. If we perform this calculation with references to Figs. 7 and 8 we find that the discrepancy is of about 3% ($m^1_{\text{w}\infty} - m^0_{\text{w}\infty} = 0.0061$ kg/m^2 instead of $m^1_{\text{w}} - m^0_{\text{w}} = 0.0064$ kg/m^2), well within the order of accuracy here considered.

Once we have estimated b_{w}, we can deduce the expected deposited mass at the end of the linear regime $m_{\text{w}}(t_0)$, to be used for the determination of D_{w}. Indeed

$$c^*_{\text{tot}} = C_{\text{s}}(T_{\text{cloud}})$$

and

$$c^*_{\mathrm{tot}} - C_{\mathrm{s}}(T_{\mathrm{b}}) = b_{\mathrm{w}}(T_{\mathrm{cloud}} - T_{\mathrm{b}}),$$

so that (2.35) yields

$$m_{\mathrm{w}}(t_0) = \frac{b_{\mathrm{w}}(T_{\mathrm{cloud}} - T_{\mathrm{b}})(R_{\mathrm{e}}^2 - R_{\mathrm{i}}^2)}{2R_{\mathrm{i}}}. \tag{3.4}$$

Exploiting (3.3) in (3.4) we get

$$m_{\mathrm{w}}(t_0) = 0.0038\ \frac{\mathrm{kg}}{\mathrm{m}^2}, \tag{3.5}$$

which is the value of deposited mass at desaturation time.

3.2. Evaluating D_w

In the linear growth phase, the deposition rate is constant and is given by

$$\dot{m}_{\mathrm{w}} = D_{\mathrm{w}} b_{\mathrm{w}} \left.\frac{\partial T}{\partial r}\right|_{R_{\mathrm{i}}}.$$

Thus

$$D_{\mathrm{w}} = \frac{m^*_{\mathrm{w}}}{t^*}\,\frac{1}{b_{\mathrm{w}}\left.\frac{\partial T}{\partial r}\right|_{R_{\mathrm{i}}}},$$

where m^*_{w} is a measure of deposited wax taken at time $t^* < t_0$, that is before desaturation (linear growth regime). From (2.22)

$$D_{\mathrm{w}} = \frac{m^*_{\mathrm{w}}}{t^*}\,\frac{k(R_{\mathrm{e}} + R_{\mathrm{i}})}{b_{\mathrm{w}} h R_{\mathrm{e}}(T_{\mathrm{e}} - T_{\mathrm{i}})}. \tag{3.6}$$

Of course (3.6) still holds at time $t = t_0$

$$D_{\mathrm{w}} = \frac{m_{\mathrm{w}}(t_0)}{t_0}\,\frac{k(R_{\mathrm{e}} + R_{\mathrm{i}})}{b_{\mathrm{w}} h R_{\mathrm{e}}(T_{\mathrm{e}} - T_{\mathrm{i}})}. \tag{3.7}$$

The desaturation time t_0 depends on D_{w}. The greater is D_{w} the smaller is t_0. From (2.14)

$$T_{\mathrm{b}}(R_{\mathrm{e}} + R_{\mathrm{i}}) - R_{\mathrm{i}}T_{\mathrm{i}} = R_{\mathrm{e}}T_{\mathrm{e}},$$

$$T_{\mathrm{e}} = \frac{1}{R_{\mathrm{e}}}[T_{\mathrm{b}}R_{\mathrm{e}} + T_{\mathrm{b}}R_{\mathrm{i}} - R_{\mathrm{i}}T_{\mathrm{i}}],$$

$$T_{\mathrm{e}} - T_{\mathrm{i}} = \frac{1}{R_{\mathrm{e}}}[(R_{\mathrm{e}} + R_{\mathrm{i}})(T_{\mathrm{b}} - T_{\mathrm{i}})],$$

so that

$$T_{\mathrm{e}} - T_{\mathrm{i}} = \frac{1}{R_{\mathrm{e}}}[(R_{\mathrm{e}} + R_{\mathrm{i}})\Delta T].$$

Formula (3.6) becomes

$$D_{\mathrm{w}} = \frac{m^*_{\mathrm{w}}}{t^*}\,\frac{k}{b_{\mathrm{w}} h \Delta T}. \tag{3.8}$$

To determine D_{w} we need to know ΔT, k, h, b_{w} and a deposition measure m^*_{w} at some time t^* less or equal than the desaturation time t_0. Surely $m^*_{\mathrm{w}} < m_{\mathrm{w}}(t_0)$ if $t^* < t_0$. Looking at Fig. 4 we see that the measure $m_{\mathrm{w}}\widehat{\Delta T}$ relative to $\widehat{\Delta T} = 4.4^{\circ}K$ is smaller than $m_{\mathrm{w}}(t_0)$. Indeed

$$m_{\mathrm{w}}\widehat{4.4^{\circ}K} = 0.0034\ \frac{\mathrm{kg}}{\mathrm{m}^2} < m_{\mathrm{w}}(t_0) = 0.0038\ \frac{\mathrm{kg}}{\mathrm{m}^2}.$$

This means that such measure is taken during the linear growth regime. Thus we evaluate wax diffusivity by means of (3.8) with $m_w^* = m_w \widehat{4.4^\circ}\mathrm{K}$, $t^* = 16h$, $\Delta T = 4.4$ K, h, k given by (2.10), (2.11) and b_w given by (3.3). We get

$$D_w \approx 4.4 \times 10^{-10}\mathrm{m}^2/\mathrm{s}. \tag{3.9}$$

At this point we may use the values of b_w *e* D_w to plot the mass growth vs time for different ΔT. We make use of (2.36) with λ given by (2.31), that is

$$m_w(t) = m_w(t_0) + \frac{b_w(R_e^2 - R_i^2)(T_b - T_i)}{2R_i}\left[1 - \exp\left(-\frac{2D_w h R_i}{k(R_e^2 - R_i^2)}(t - t_0)\right)\right]. \tag{3.10}$$

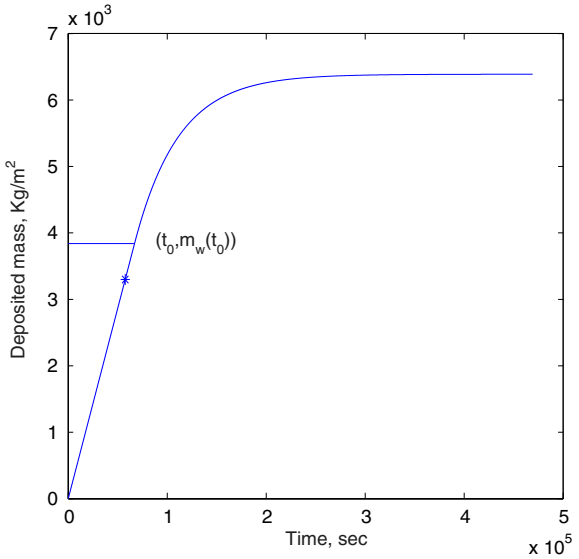

Fig. 5. $\Delta T = 4.4$ K, $t_0 \approx 18$ h.

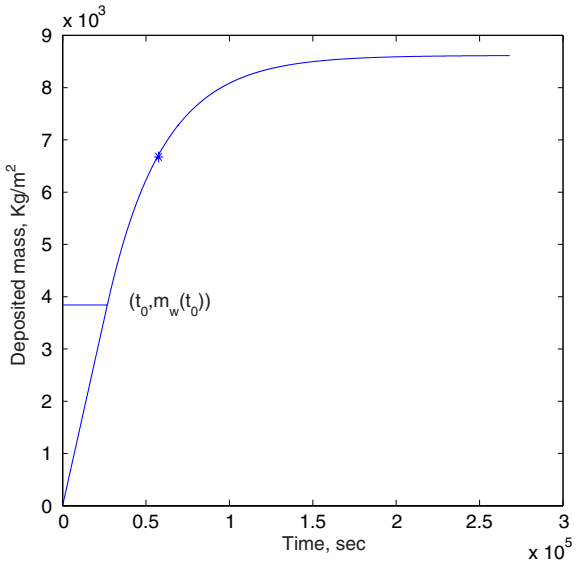

Fig. 6. $\Delta T = 8.3$ K, $t_0 \approx 7$ h.

We notice that the wax diffusivity D_w depends on the heat-transfer model used to determine h (see (3.8)) whereas the relevant quantity for predicting mass deposit (besides b_w) is the product $D_w h$. A different heat-transfer model would produce different h and D_w, the product $D_w h$ remaining the same. Of course this is a delicate point of the model since there is no general agreement on the way of determining the heat transfer coefficient h.

Formula (3.10) allows to validate our original guess for b_w. Growth curves are shown in Figs. 5–8. Continuous lines are plotted using (3.10), while stars represent experimental mass measures at 16 h. The point $(t_0, m_w(t_0))$ is also plotted. We notice that only the measure with $\Delta T = 4.4$ K is in the linear stage and that the desaturation time decreases as ΔT increases. We remark however that formula (3.10) with the values of b_w, D_w deduced using the three sets of data $\Delta\ T = 4.4$ K, $\Delta T = 13.8$ K, $\Delta T = 25$ K actually fits the fourth datum $\Delta T = 8.3$ K very nicely (see Fig. 7). This is an additional validation of the model.

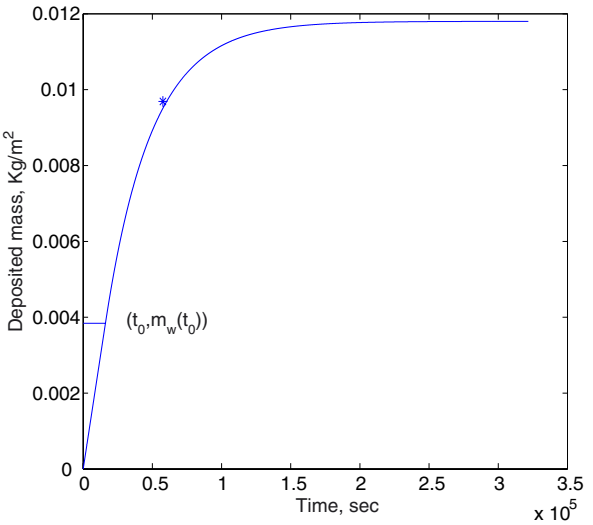

Fig. 7. $\Delta T = 13.8$ K, $t_0 \approx 4$ h.

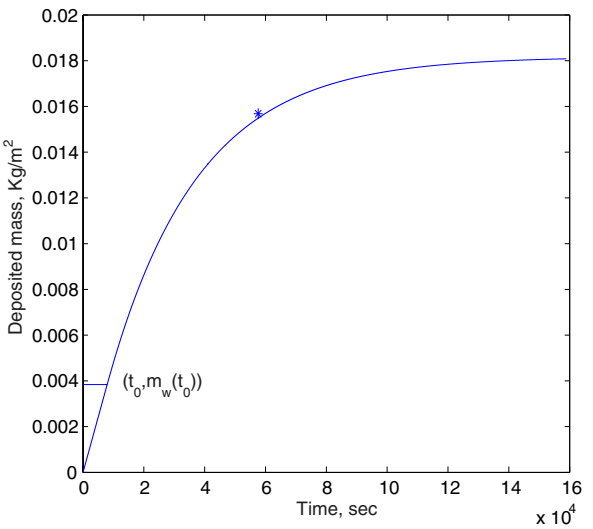

Fig. 8. $\Delta T = 25$ K, $t_0 \approx 2$ h.

Other experimental data, unfortunately limited to the unique measure for a temperature difference between the warm and the cold wall of 17 K can be found in [9]. Of course b_w cannot be evaluated since we need at least two different asymptotic mass measures. However, if we use a typical value $b_w \approx 0.015$ kg/(m^3 K) we find $D_w \approx 3.5 \times 10^{-10}$ m^2/s.

4. Conclusions

We have presented a model for wax deposition in a cold finger device with oil stirring. The model allows to determine wax solubility and diffusivity from experimental measurements. Such parameters are of crucial importance for determining deposition rates in pipelines. The transfer of dissolved wax towards the cold finger wall (driven by molecular diffusion) takes place in a boundary layer where the temperature profile is calculated in terms of the geometry of the device and of the heat transfer coefficient (expressed as a function of the stirring speed and of the physical properties of the oil).

The formation of the deposit is discussed as a two-stage process. In the first stage the oil is saturated by wax and in the second stage is not. The model predicts that the deposition rate is constant during the first stage and allows to compute the time of transition to the second stage. The evolution of wax concentration during the unsaturated regime is calculated, showing that the mass of solid wax deposited tends exponentially to its asymptotic limit. Using the experimental data of [3] we deduce reliable values for wax solubility and diffusivity, on the basis of which the growth of the deposit can be predicted in given experimental conditions.

Although the number of data we have used is small, we could exploit the fortunate circumstance that two of them fall close to the asymptotic regime and one in the linear growth regime. This was enough to start the procedure of evaluation of the desired quantities and eventually to validate the model on the basis of further verifications.

References

[1] S. Correra, M. Andrei, C. Carniani, Wax diffusivity: is it a physical property or a pivotable parameter? Petrol. Sci. Technol. 21 (9) (2003) 1539–1554.
[2] S. Correra, A. Fasano, L. Fusi, M. Primicerio, F. Rosso. Wax diffusivity under given thermal gradient: a mathematical model, to appear on ZAMM.
[3] K. Weispfennig, D.W. Jennings, Effects of shear and temperature on wax deposition: cold finger investigation with a GOM crude oil, The 5th International Conference on Petroleum Phase Behaviour and Fouling, June 13–17(2004).
[4] Chien-Hou Wu, J.L. Creek, Kang-Shi Wang, R.M. Carlson, S. Cheung, P.J. Shuler, Yongchun Tang, Measurments of wax deposition in paraffin solutions, prepared for presentation at the 2002 Spring National Meeting, New Orleans, March 10–14, Wax Thermodynamic and Deposition.
[5] L.F.A. Azevedo, A.M. Teixeira, A critical review of the modeling of wax deposition mechanisms, Petrol. Sci. Technol. 21 (3& 4) (2003) 393–408.
[6] E.D. Burger, T.K. Perkins, J.H. Striegler, Studies of wax deposition in the trans Alaska pipeline, J. Petrol. Technol. (June) (1981) 1075–1086.
[7] P. Singh, R. Venkatesan, H. Scott Fogler, N.R. Nagarajan, Morphological evolution of thick wax deposits during aging, AIChE J. 47 (1) (2001) 6–18.
[8] K. Weispfennig, Advances in paraffin testing methodology. SPE 64997 (2001).
[9] K. Weispfennig, D.W. Jennings, Paraffin deposition modeling using benchtop deposition tests. AIChE Spring National Meeting (March) (2002) New Orleans LA.